ACS APPLIED MATERIALS & INTERFACES

Research Article

www.acsami.org

Effect of Nanoclay Loading on the Thermal and Mechanical Properties of Biodegradable Polylactide/Poly[(butylene succinate)-co-adipate] Blend Composites

Vincent Ojijo,[†,‡] Suprakas Sinha Ray,[†,§,*] and Rotimi Sadiku[‡]

[†]DST/CSIR NIC, National Centre for Nano-Structured Materials, Council for Scientific and Industrial Research, 1-Meiring Naude Road, Brummeria, Pretoria 0001, South Africa

[‡]Division of Polymer Technology, Department of Mechanical Engineering, Tshwane University of Technology, Pretoria 0001, South Africa

[§]Department of Chemical Technology, University of Johannesburg, Doornfontein 2018, Johannesburg, South Africa

Supporting Information

ABSTRACT: Polylactide/poly[(butylene succinate)-co-adipate] (PLA/PBSA)-organoclay composites were prepared via melt compounding in a batch mixer. The weight ratio of PLA to PBSA was kept at 70:30, while the weight fraction of the organoclay was varied from 0 to 9%. Small angle X-ray scattering patterns showed slightly better dispersion in PBSA than PLA, and there was a tendency of the silicate layers to delaminate in PBSA at low clay content. Thermal analysis revealed that crystallinity was dependent on the clay content as well its localization within the composite. On the other hand, thermal stability marginally improved for composites with <2 wt % clay content in contrast to the deterioration observed in composites with clay content >2 wt %. Tensile properties showed dependence on clay content and localization. Composite with 2 wt % clay content showed slight improvement in elongation at break. Overall, the optimum property was found for a composite with 2 wt % of the organoclay. This paper therefore has demonstrated the significance of the clay content and localization on the properties of the PLA/PBSA blends.

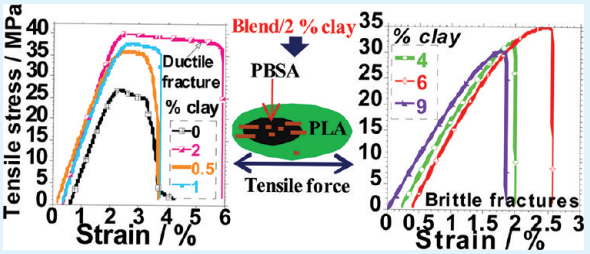

KEYWORDS: *clay loading, morphology, PLA/PBSA blend, properties*

1. INTRODUCTION

Being a biodegradable and biocompatible polymer, polylactide (PLA) has found a number of uses, mainly in biomedical applications and as an advanced environmentally benign material.[1,2] The possibility of it being produced from annually renewable resources has also fostered increased interest in it. However, despite having good properties like biodegradability and high strength, its low flexibility and low impact strength[3] limit its applications. It is therefore imperative that the brittleness of PLA be reduced in order to allow for more practical applications such as environmentally friendly packaging.

The brittleness could be overcome through blending PLA with more ductile and still biodegradable polymers such as polycaprolactone (PCL),[4−7] poly(butylene adipate-*co*-tephthalate),[8] and poly[(butylene succinate)-*co*-adipate] (PBSA).[3,9,10] In the current study, the ductile PBSA has been used to modify the properties of PLA. In the preparation of such blends, it is desirable that specific properties from the different polymers be combined into one material through a blending process that is relatively simple and cheaper than the synthesis of a new material. However, because of the immiscibility of some of the polymer blends, phase separation usually occurs, which leads to probable deterioration of properties, instead of the envisaged improvement. Therefore, the control of phase morphology of such blends is paramount if proper balance of properties is to be achieved.[11,12]

The traditional route of compatibilization of thermodynamically immiscible blends has been through the application of several methods such as the use of block and graft copolymers which strengthen the interface and stabilize the morphology.[13,14] However, they are system specific, relatively expensive to engineer and difficult to produce for systems with more than two components.[11] There are other novel ways of stabilizing the blend morphology through use of readily available and cheap organically modified clays. Through the application of the well-established polymer/clay nanocomposite technology,[15] it is envisaged that apart from stabilisation of the blend morphology, clays would influence the properties of the polymer blends. Several authors[16] and one of the authors of the current work[17] have already demonstrated that clay can be used to enhance the morphology of polymer blends and hence a similar strategy can be used to improve the properties of PLA/PBSA blends.

Received: December 28, 2011
Accepted: April 11, 2012
Published: April 11, 2012

Indeed, in a previous work,[10] pristine montmorrillonite (MMT) and four organically modified MMTs (OMMTs) were investigated for their ability to influence the morphology and hence the properties of PLA/PBSA blend. The clay interlayer spacing, the concentration of the modifier on the clay surface, and the miscibility between the polymers and the surfactant were found to influence the resulting morphology and hence the properties. However, with the fixed clay content (6 wt %) used in that study, it was not possible to appreciate the full spectrum of morphological and hence property evolution with different clay concentrations. In a continuation of the work, an organically modified clay containing-blend with the finest morphology and hence the best and balanced properties was chosen for further investigation by varying the organoclay concentration from 0 to 9 wt %.

Blends of PLA/polymer/clay at various clay concentrations have been investigated before. Yu et al.[18] investigated the role of organically modified clay in enhancement of tensile strength, modulus, and elongation at break for PLLA/PCL-clay nanocomposites. Depending on the clay content, the mechanical properties were either enhanced or reduced. Likewise, Chen and co-workers[19,20] compared the influence of organically modified clay and twice functionalized clay on the morphology and properties of PLLA/poly(butylene succinate) and PLLA/poly(butylene succinate-*co*-butylene adipate) blends. In each case, they reported enhancement of certain properties such as modulus and thermal stability with increase in clay loading, while improvement for elongation at break and yield strength depended on the clay loading and clay functionalization. More recently, Li et al.[7] investigated thermal and biodegradability of PLA/PCL compounded with functionalized organoclay. The epoxy-functionalized organoclay dispersed more in the polymer matrix than the as-obtained organoclay, thereby resulting in better thermal stability and greater degradation when composted.

It needs to be recognized that due to a number of reasons, there could be preferential localization of the third component in the blends of polymers/inclusion in either of the two polymers.[6,21] However, to the best of our knowledge, we did not find work on the clay localization within either component of the PLA/PBSA blend at different concentrations or how this affects the properties of the composites reported in the literature. This work, therefore, reports on the influence of the clay loading on the morphological evolution and thermal and mechanical properties of the PLA/PBSA blend composites. The objective of the work was to try to optimize the clay concentration in the blend so as to get the best properties from both polymers, especially the ductility of PBSA.

2. EXPERIMENTAL SECTION

2.1. Materials. The PLA used in the study is a commercial grade (PLA 2002D), obtained from Natureworks LLC, USA. It had a D-isomer content of about 4%; weight average molecular weight, M_w = 235 kg/mol; density = 1.24 g/cm^3; glass transition temperature, $T_g \approx$ 60 °C; and melting temperature, $T_m \approx$ 153 °C. On the other hand, the PBSA, with the designation BIONOLLE #3001, was obtained from Showa High Polymer (Japan). According to the supplier, it had M_w = 190 kg/mol, density =1.23 g/cm^3 (ASTM 1238), T_g = −43.8 °C, and T_m's = 83.1 °C (first) and 94.5 °C (second). Before use, PLA was dried at 60 °C under a vacuum for 36 h, whereas PBSA was dried at 60 °C under a vacuum for 12 h.

The organically modified clay, Cloisite®C20A (C20A), was obtained from Southern Clay Products, Inc. It had been synthesized by cation exchange reaction between Na^+ in pristine MMT with quaternary ammonium salt, with the resulting surfactant concentration of 95 meq/100 g clay and a reported interlayer spacing of 2.42 nm.[22] This clay was chosen for the current study since it had the optimal performance, in terms of the control of PLA/PBSA morphology and the resulting properties when compared to others investigated in our previous work.[10]

2.2. Preparation of Polymer Blend and Blend−Clay Composites. Dried pellets of PLA and PBSA in the ratio of 70:30 were mixed. This ratio was chosen since PLA was our target polymer, whose properties were to be improved and the ratio also resulted in a good balance of properties. Prior to the melt-blending process, the blend was mixed with different weights of C20A in a bag: 0.5, 1, 2, 4, 6, and 9 wt.%. The mixture was melt-blended in a HAAKE PolyLab OS Rheomix (Thermo Electron Co., USA) operated at a rotor speed of 60 rpm, at a temperature of 185 °C (set temperature) for 8 min. The blend and the composites were then compression molded using a Carver laboratory press at 185 °C and cooled to room temperature. The composites prepared were labelled: B, B0.5, B1, B2, B4, B6, and B9 for composites with 0, 0.5, 1, 2, 4, 6, and 9 wt % C20A contents, respectively.

To study the specific interaction between the PLA and PBSA individually with the organoclay, composites of PLA-clay and PBSA-clay were prepared in the same way and condition as the blend-clay composites. The PLA composites containing 2 and 6 wt % clay content were denoted PLA2 and PLA6, respectively. On the other hand, PBSA composites containing 2 and 6 wt % clay content were denoted PBSA2 and PBSA6, respectively.

2.3. Characterization and Property Measurements. Small-angle X-ray scattering (SAXS) studies were carried out to investigate the dispersion of clay particles in the neat polymer and blend composites. The SAXS analyses were carried out with an Anton Paar SAXSess instrument, operated at 40 kV and 50 mA with line collimation geometry. A CuKα radiation with a wavelength of 0.154 nm (PANalytical X-ray source) was used. The intensity profiles were obtained with line collimated SAXSess and recorded with a 2D-imaging plate. The sample-to-detector distance was 261.2 mm, and the radius of detector curvature was 260 mm. The read-out angles were calculated from the pixel size and the obtained q-scale was cross-checked by measuring silver behenate whose equidistant peak positions are known. The exposure time for each experiment was 5 min. The samples used were thin films prepared through compression molding.

Differential scanning calorimeter (DSC) measurements were carried out on a DSC-Q2000 instrument (TA Instruments) under Helium atmosphere using approximately 11.7 mg of samples. The thermal properties of neat polymers and their neat blend were investigated by initially heating the samples at 10 °C/min to 190 °C to destroy the thermal histories. Thereafter, cooling was carried out at different rates: 20, 10, 5, 2.5, and 1 °C/min from 190 °C to −65 °C for PBSA and neat blend and 15 °C for PLA. A second heating was then done at 10 °C/min to 190 °C. For the composites, the cooling rate was kept at 20 °C/min, whereas the heating rate was 10 °C/min. All composite samples were weighed in such a way that the amount of polymer matrix was the same.

The thermal stability of the neat polymer, neat blend, and blend composites was determined by means of thermogravimetric analyzer using a TGA Q500 (TA Instruments) at a heating rate of 10 °C under air atmosphere, from room temperature to 900 °C. Samples were approximately 3.8 mg, and all the tabulated TGA results are the average of three independent measurements.

Tensile properties, such as modulus, yield strength, and elongation at break of neat polymers, neat blend, and blend−clay composites, were determined using Instron 5966 tester (Instron Engineering Corporation, USA) with a load cell of 10 kN. This was carried out under tension mode at a single strain rate of 5 mm/min at room temperature. Dog bone shaped samples had previously been annealed at 80 °C for 15 h under vacuum. The results presented are an average of at least six independent tests.

3. RESULTS AND DISCUSSION

3.1. Structural Elucidation by SAXS. The dispersion of clay in PLA and PBSA was studied through SAXS. To investigate the thermodynamic interaction between the individual polymers and the organoclay, we carried out SAXS measurement on PLA−clay and PBSA−clay composites prepared in the same way, and the results are shown in Figure 1.

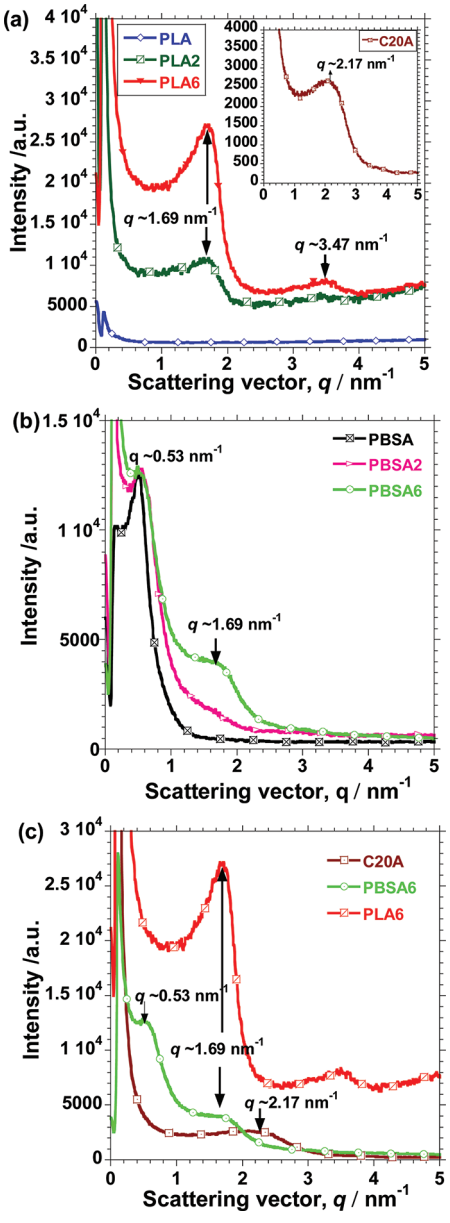

Figure 1. SAXS patterns of (a) C20A, PLA, and PLA-clay composites; (b) PBSA and PBSA-clay composites; and (c) C20A, PLA6, and PBSA6.

The characteristic scattering vector of C20A $q \approx 2.17$ nm^{-1} corresponded to the interlayer spacing of $d_{(001)}$= 2.90 nm (refer to the inset in Figure 1a). After melt compounding of 2 and 6 wt % C20A with PLA, this characteristic peak of C20A shifted to a lower value of ~1.69 nm^{-1}, corresponding to the interlayer spacing of 3.72 nm. The increase in the interlayer spacing was attributed to the intercalation of PLA molecules into the clay galleries. The higher order peak ($d_{(002)}$) appeared at a scattering of $q \approx 3.47$ nm^{-1} in the PLA-clay composites as shown in Figure 1a. This corresponded to a d-spacing of about 1.81 nm, making the two peaks almost an integral multiple of each other. These results signify that these two peaks arise from the same periodic structural source of C20A.

In Figure 1b, it is observed that PBSA has a peak in the very low scattering vector region of q = 0.53 nm^{-1} attributable to the existence of periodicity of polymer chains. Nevertheless, for the PBSA composites with 6 wt % clay content (PBSA6), a shoulder appears in a position almost similar to characteristic $d_{(001)}$ peak of C20A observed in PLA6: $q \approx 1.69$ nm^{-1}, even though the intensity is not as much. In fact, for the PBSA composite with 2 wt % clay (PBSA2), the peak is almost absent. Even though the near absence of the characteristic peak in PBSA2 when compared to PLA2 could be due to the difference in the sample thickness, it could also be due to the probable disorder arising from delaminated clay platelets in PBSA2. The viscosity of PBSA at 185 °C is much lower than that of PLA and diffusion of its molecules into the clay galleries would therefore be much easier, thus encouraging intercalation and delamination. Moreover, as shown in Figure 1c, the broad shoulder of the PBSA-clay composite peak around q = 1.69 nm^{-1}, as opposed to the sharper peak for PLA−clay composite at a similar position, may be due to the slightly better intercalation of PBSA as well as delamination due to its lower viscosity. However, we contend that the enthalpic interaction between PLA and PBSA with the C20A clay is not so different; hence the appearance of the weak peak at a scattering vector of $q \approx 1.69$ nm^{-1} in the PBSA6 sample was almost similar to that of PLA6.

To understand the dispersion of clay in the blend, SAXS studies were done on composites with different clay content, and the results are shown in Figure 2. At low clay concentration (0−2 wt %), hardly any peak is visible. At 1 wt % clay content, just a small shoulder was observed. The shoulder at $q \approx 1.57$ nm^{-1} becomes slightly more prominent in the composite with 2 wt % clay. The characteristic peak at $q \approx 1.57$ nm^{-1} corresponds to an interlayer spacing of 4.0 nm, representing a 38% increase over that of neat C20A. This observation is consistent with what was observed in PBSA with 2 wt.% clay as shown in Figure 1b. This implies that at low clay concentration, PBSA could be the polymer intercalating the clay, and not PLA. The intercalation by PBSA alone, however, is only realized until the clay concentration of 2 wt %. Above 2 wt %, a more prominent characteristic peak is observed for all the samples approximately at a similar scattering vector of $q \approx 1.69$, corresponding to an interlayer spacing of 3.72 nm. This represented a 28% increase in the interlayer spacing of clay in the composites over the neat C20A clay. This is strikingly similar to the increase in interlayer spacing in the case of PLA/clay composites and PBSA composite with 6 wt.% clay in Figure 1. This would imply that above 2 wt %, clay was intercalated by both PLA and PBSA. Indeed, previous surface morphological and transmission electron microscopy studies (refer to the Supporting Information, Figures S1 and S2)[23] revealed localization of clay within the PBSA phase at concentrations less than 2 wt %. Hence the 2 wt % can be seen as a threshold concentration when clay moves into PLA phase, stabilizing the morphology of the composite. This unique behavior, therefore, results in categorization of the composites into three groups: (i) regime 1, when clay sits within PBSA (B0.5 and B1); (ii) regime 2, the transitional regime when clay sits at the interface, as well as within both PLA and PBSA (B2),

dx.doi.org/10.1021/am201850m | ACS Appl. Mater. Interfaces 2012, 4, 2395−2405

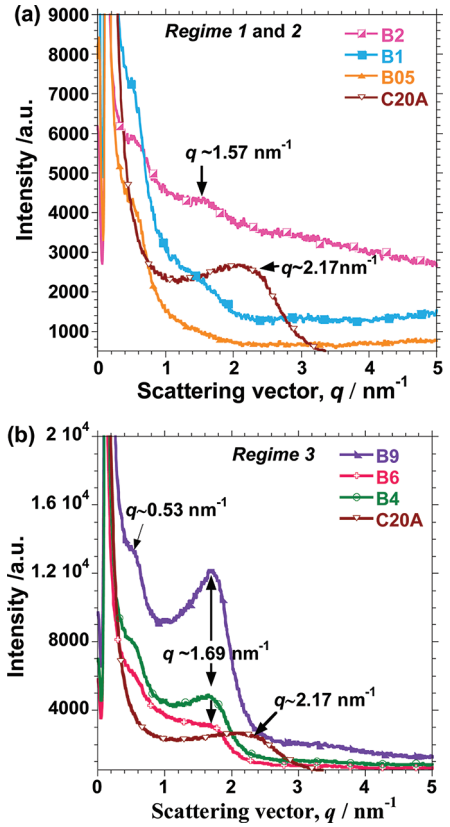

Figure 2. SAXS patterns of C20A and blend–clay composites in (a) regime 1 and 2 (B05, B1, and B2) composites and (b) regime 3 (B4, B6, and B9) composites. B, neat blend; B0.5, B1, B2, B4, B6, and B9 are composites with 0.5, 1, 2, 4, 6, and 9 wt % clay, respectively.

and (iii) regime 3, when clay increasingly resides within PLA phase (B4, B6, and B9).

The slightly higher interlayer spacing of clay in the regime 1 and 2 composites (4.0 nm) when compared to that of the regime 3 composites (3.72 nm) could be attributed to two factors: (i) low viscosity of PBSA allowing easier diffusion of molecules into the galleries of clay and hence a larger extent of intercalation, and (ii) common intercalation of both PLA and PBSA into the galleries of the clay particles sitting at the interface of the two polymers (refer to the Supporting Information).

The melt flow properties of the composites better illustrates the influence of the clay loading. Figure 3 shows the clay

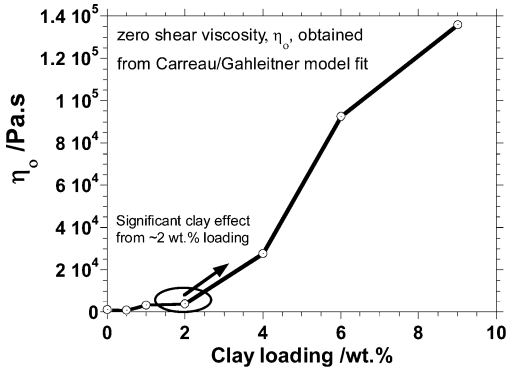

Figure 3. Clay loading dependence of zero shear viscosity.

loading dependence of zero shear viscosity. A significant increase in the zero shear viscosity (predicted from Carreau/Gahleitner model[24]) was realized only after 2 wt % clay content. At low clay content (< 2 wt %), the clay resided within PBSA phase and hardly participated in the increase of the viscosity of PLA, which was the major phase, until after 2 wt % clay loading.

From the SAXS studies, it is expected that the behavior of the composites with regards to thermal and mechanical properties will be different and confined to the different regimes, because of the localization of clay.

3.2. Differential Scanning Calorimetry. DSC was used to study the thermal properties of the neat blend and blend-clay composites. The neat PLA had a very slow crystallization rate and there was hardly any melting enthalpy registered even after cooling at 1 °C/min (refer to the Supporting Information, Figure S3). On the other hand, the neat PBSA showed sharp crystallization peaks when cooled at a different rate (1–20 °C/min) (refer to the Supporting Information, Figure S4). In the neat PLA/PBSA blend, unique thermal events, different from those observed in the individual components, occurred. Figure 6 (a) shows multiple crystallization exotherms for PBSA component, whereas there was none for PLA (no exotherm the T_g of PLA, 60 °C).

The occurrence of the multiple crystallization peaks (ranging from −3.6 to 64.2 °C) of the minor phase PBSA is attributed to the fractionated crystallization phenomenon, which occurs when the number of droplets of the minor phase is higher than the number of heterogeneities that act as nuclei[25] and has been observed for a number of systems, e.g., in polypropylene/poly(ε-caprolactone) blends[26] and even in PLA/PBSA blends.[9]

On the other hand, the thermal events in the heating scan in part b of Figure 4 shows a glass transition temperature at ∼57 °C; melt endotherms of PBSA at ∼94 °C; distinct cold crystallization exotherms for PLA with peaks ranging from 117.3–118.7 °C, and melt endotherms for PLA components with single peaks at about 148 °C. When compared with neat PLA with T_{cc} of 131 °C, the T_{cc} of PLA in the neat blend decreased significantly to ∼118°C. It is considered that PBSA acted as a nucleating agent for PLA during the cooling process, and hence the pre-formed crystal nuclei were able to cold crystallize at a lower temperature than that of neat PLA.

The fractionated crystallization phenomenon was further investigated through polarized optical microscopy. This was done by monitoring the spherulites evolution in the neat blend during the cooling run (at 2.5 °C/min), from melt phase (∼175 °C) to room temperature (∼25 °C). A correlation was made between the DSC results in Figure 4a and the temperature-dependent spherulite development, as observed by POM. Figure 5 shows the DSC cooling curve of neat PLA/PBSA blend and POM micrographs depicting the typical spherulite development at different temperatures during cooling. In part (b) of Figure 5, a phase separated structure is clearly observed in the melt-phase with the continuous phase being PLA and the dispersed phase being PBSA. This further confirms the immiscibility of the two polymers.

On cooling the blend from melt-phase at 2.5 °C/min, only PBSA was observed to crystallize as the cooling rate was seemingly high for the crystallization of PLA (refer to the Supporting Information, Figures S3 and S4). As shown in parts c and d of Figure 5, the first batch of ring-banded PBSA spherulites grew in the temperature region of 61–65 °C. A closer inspection of the ring banded spherulites reveals that

dx.doi.org/10.1021/am201850m | ACS Appl. Mater. Interfaces 2012, 4, 2395–2405

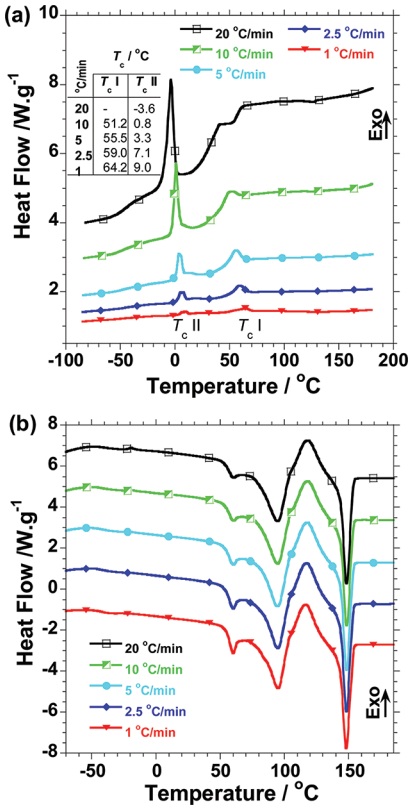

°C/min	T_c I	T_c II
20	-	-3.6
10	51.2	0.8
5	55.5	3.3
2.5	59.0	7.1
1	64.2	9.0

Figure 4. DSC curves of PLA/PBSA neat blend (a) on cooling from melt at 1 to 20 °C/min and (b) on heating at 10 °C/min, following cooling at different rates indicated on the graph: 1 to 20 °C/min. For clarity, data were vertically offset.

their epicenters were mostly at the PLA/PBSA interphase. This implies that there was a kind of heterogeneous nucleation occurring on the mostly amorphous PLA surface. The spherulites formed in this temperature region obviously corresponded to the first crystallization peak observed in part a of Figure 5.

On further cooling to approximately 53 °C, the hitherto uncrystallized big PBSA phase crystallizes into somewhat large single spherulites. The spherulites seemed to grow laterally within the confines of the PBSA phase. It is speculated at this point that there was heterogeneous nucleation of PBSA just like in the first instance, but this time lower activation energy was required. We propose that the subsequent heterogeneous nucleation might have resulted from the glass slides used, between which the samples were imbedded during POM studies. It is probable that the energy required to activate the glass surface as a nucleating site for PBSA was lower than that of the amorphous PLA surface. In the DSC cooling scan in part a of Figure 5, crystallization of the PBSA at 53 °C and those crystals formed in the 65 °C region are both represented by the first crystallization peak observed at around 60 °C.

Further cooling of the blend to 30 °C results in emergence of numerous and well rounded spherulites (refer to Figure 5f) that correspond to the crystallization peak observed at approximately 20 °C in the DSC cooling scan shown in Figure 5a. However, because the POM hot stage could not be cooled to lower temperatures, it was not possible to verify the homogenous nucleation expected at around 7 °C. Even though the mechanism of heterogeneous nucleation at around 20 °C is not known, the POM results have, however, successfully confirmed the fractionated crystallization phenomenon of PBSA observed during cooling as depicted in part a of Figure 4.

In the case of composites, thermograms obtained while heating at 20 °C/min following a 20 °C/min cooling process were used to illustrate the effect of clay loading. The DSC heating scan of the composites shown in Figure 6 revealed a number of thermal events: distinct cold crystallization exotherms for both PBSA phase and PLA phases; clear T_g for PLA at ∼57 °C; single melting endotherm for PBSA and multiple PLA melting endotherms except for B2 and B6 samples. The fractionated crystallization of PBSA phase was equally observed in the composites cooled at different temperatures, although the graphs are not shown here.

The presence of distinct cold crystallization exotherms for PBSA in the blend composites, unlike in the neat polymers (refer to the Supporting Information, Figure S3) or neat PLA/PBSA blend (refer to Figure 4b), cooled at a similar rate, indicates that the clay impeded crystallization of PBSA on cooling from melt-state. The crystallization of PBSA becomes more pronounced only when the sample is heated again. The cold crystallization exotherms tended to be enhanced with the addition of clay, while the cold crystallization temperature generally increased with the addition of clay too. This implies that during the cooling cycle, increased clay content must have acted as a physical barrier for crystal growth. Even though the determination of the melt enthalpy for the PBSA component was tricky because of the difficulty in choosing the baseline, there was only one melting point at ∼94 °C for PBSA component in all the composites, just like in the case of neat blend.

However, for the PLA component, a different melt phenomenon was observed depending on the clay loading and localization and the morphology of the composites. The melt behavior in the composites could be explained bearing in mind the established regimes of clay localization: regime 1, 2, and 3. Generally, there was a reduction in the cold crystallization temperature with an increase in clay loading, except for 2 and 6 wt %. The cold crystallization temperature for the PLA component in a neat PLA/PBSA blend was about 118.7 °C. On introduction of 0.5 wt % clay into the blend, the cold crystallization temperature was shifted to a lower value of about 112.6 °C. The temperature then shifted to higher value of 117.8 °C for the transitional regime sample, B2. At 2 wt %, clay was not only located within both polymers, but also at the interface. It has been argued previously[23] that for the clay sitting at the interface, the common adsorption of both polymers onto the clay surface could potentially increase the crystallization activation energy, thereby limiting crystallization on cooling.

In the regime 3 samples, sustained clay loading into the PLA phase provided nucleation sites and it was expected that crystallization during cooling would be somewhat better, compared to regime 1 and 2 samples. Cold crystallization is influenced by the existing preformed crystals and in this case the more the nuclei preformed during cooling, the lower the cold crystallization temperature. Indeed, within regime 3, the cold crystallization temperature tended to decrease with the increase in clay content, and hence the nuclei density: 111.2 and 108.9 °C for B4 and B9, respectively, with the exception of the B6 sample, which was about 119.5 °C. The unique composite of 6 wt % clay loading was shown to have a co-continuous morphology, and it is assumed that the interconnectedness of the PLA with PBSA slowed down the

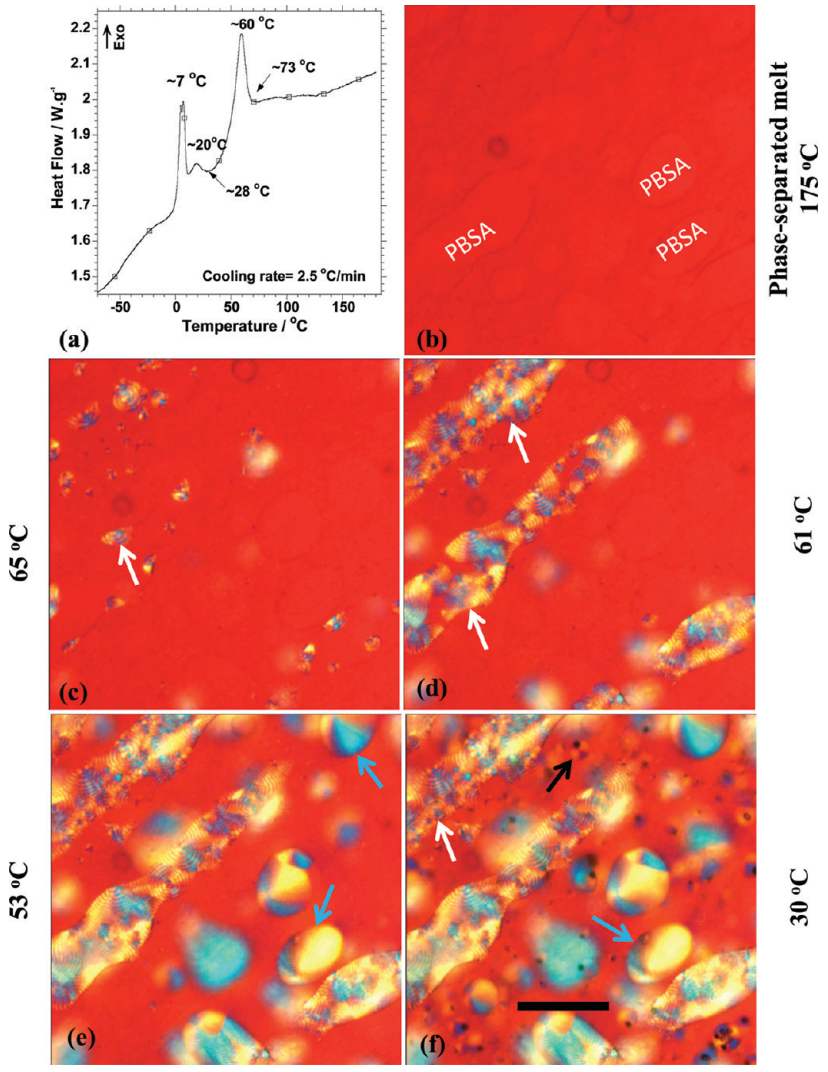

Figure 5. Fractionated crystallization of PBSA phase in the neat PLA/PBSA during cooling run (a) DSC cooling curve showing multiple PBSA crystallization peaks and none for PLA, (b–f) POM micrographs showing PBSA spherulites evolutions at the indicated temperatures: (b) melt at 175 °C with clear phase separation; (c, d) formation of PBSA spherulites with concentric extinction bands in the region of 61–65 °C corresponding to crystallization peak around 60 °C in a; (e) formation of single PBSA spherulites, taking up the remaining big PBSA phase, which until then were amorphous and (f) sprout-up of numerous smaller spherulites, corresponding crystallization peaks around 20 °C in a. Cooling rate during POM and DSC studies was the same: 2.5 °C/min. The scale bar = 99.9 μm.

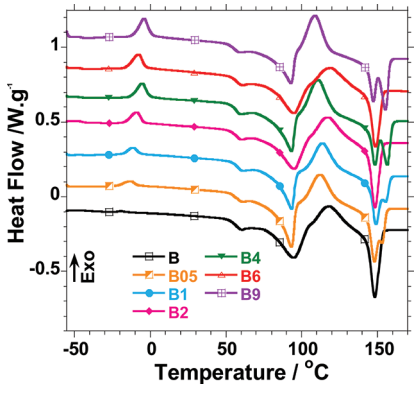

Figure 6. DSC curves of PLA/PBSA-C20A composites on heating at 10 °C/min, following cooling at 20 °C/min. B, neat blend; B0.5, B1, B2, B4, B6, and B9 are composites with 0.5, 1, 2, 4, 6, and 9 wt % clay, respectively. For clarity, data were vertically offset.

crystal formation and growth. Therefore, it is assumed that crystals were formed on cooling, and hence the higher cold crystallization temperature on heating.

Single melting peaks were observed for B, B2, and B6 specimens as opposed to the double melting peaks in B0.5, B1, B4, and B9 specimens. The double melting peaks are more pronounced in composites with 4 and 9 wt % clay, than those with 0.5 and 1 wt % clay. This could be because of the imperfections in the crystals formed when the nuclei density was high (B4 and B9), which occasioned the melting and re-crystallization of the imperfect crystal thereby resulting in the double peaks. For the B2 and B6 samples, increased crystallization activation energy limited the nucleation sites and hence the few nuclei formed tended to grow fully, albeit slowly, and hence the single melting peak.

In conclusion, it has been shown how clay inclusion alters the thermal properties of the PLA and PBSA components in the composites, depending on the location and quantity. This is expected to, likewise, affect the mechanical properties of the composites.

dx.doi.org/10.1021/am201850m | ACS Appl. Mater. Interfaces 2012, 4, 2395–2405

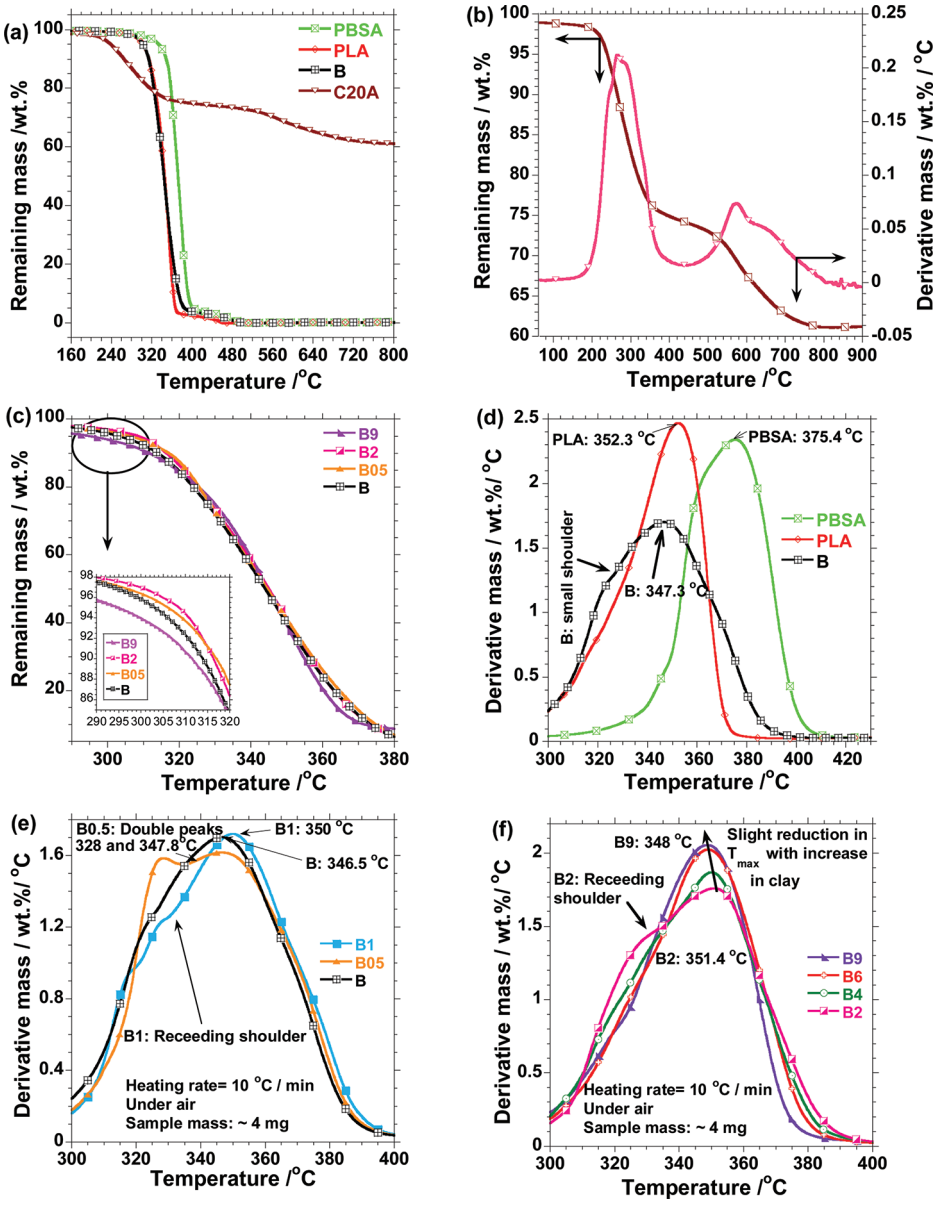

Figure 7. (a) Typical TGA thermograms PLA, PBSA, C20A, and neat blend; (b) TGA thermogram and first derivative TGA (dTGA) curve of C20A; (c) TGA thermograms of neat blend and selected composites: B05, B2, and B9; and (d–f) first derivative TGA (dTGA) curves of PLA, PBSA, neat blend, and blend–clay composites.

3.3. Thermogravimetric Analysis. Thermoxidative degradation analyses were performed on the neat polymers, neat blend, and blend-clay composites, and typical results are shown in Figure 7. The TGA thermograms of PLA, PBSA, neat blend, and C20A are shown in Figure 7a. For clarity, only selected TGA thermograms of composites from each regime (B05, B2, and B9) are illustrated in Figure 7c. In addition, for clearer visualization of thermal stability, the first derivative TGA (dTGA) curves of the neat polymers, neat blend, and blend-clay composites are shown in Figure 7d–f. Finally, Table 1 gives a summary of TGA data: (i) onset degradation temperature, T_5, taken arbitrarily as the temperature at which 5% degradation occurred; (ii) T_{max}, the temperature at which maximum rate of degradation occurred; and (iii) the percentage char formation at 600 °C, all reported as averages of three independent tests.

Figure 7a shows that PBSA is more thermally stable than PLA. On blending PLA with the more thermally stable PBSA, not much difference in the stability of the blend when compared to neat PLA was noted. On the other hand, C20A shows a multiple-step degradation process, with the initial rapid step occurring between 180 to 380 °C (refer to Figure 7b). Thereafter, a much slower rate of degradation occurs in the region between 380 and 500 °C. Above 500 °C, the degradation continues at a slower rate until only the inorganic silicates (38%) are left at around 800 °C.

Because inorganic substances have good thermal stability, it is generally believed that the introduction of layered silicate platelets into organic materials can improve their thermal stability. This is because, not only do they act as a heat barrier in the early stages of thermal decomposition, but they also slow down the volatilization due to the labyrinth effect they create in the polymer composites.[27] The thermal stability of the composites was not only dependent on the concentration of clay but also on its localization and the resulting morphology.

dx.doi.org/10.1021/am201850m | ACS Appl. Mater. Interfaces 2012, 4, 2395–2405

Table 1. Onset Degradation Temperature at 5% Weight Loss (T_5), Temperature at Maximum Degradation Rate (T_{max}), and % Char Formation at 600 °C for Neat Polymers, Blend, and Blend−Clay Composites[a]

	T_5 (°C)		T_{max} (°C)		char at 600 (%)	
sample[b]	mean	s.d.	mean	s.d.	mean	s.d.
PLA	303.4	(1.4)	352.9	(0.6)	0.02	(0.03)
PBSA	333.9	(0.9)	376.3	(2.3)	0.02	(0.03)
B	306.7	(3.2)	347.4	(1.7)	0.04	(0.02)
B0.5	307.7	(1.7)	348.5	(0.6)	0.23	(0.10)
B1	307.2	(3.2)	351.0	(1.0)	0.45	(0.07)
B2	307.2	(1.6)	351.8	(1.2)	1.13	(0.05)
B4	299.9	(1.9)	349.6	(0.8)	2.62	(0.35)
B6	301.7	(3.6)	349.7	(0.9)	3.17	(0.03)
B9	295.6	(0.9)	348.6	(0.1)	4.89	(0.21)

[a]Mean values of three independent tests; s.d. = standard deviation. [b]B, neat blend; B0.5, B1, B2, B4, B6, and B9 are composites with 0.5, 1, 2, 4, 6, and 9 wt % clay, respectively.

In the regimes 1 and 2, there was only a marginal improvement in the onset degradation temperatures compared to those of neat PLA and neat blend as shown in Table 1. However, further increase in clay in the regime 3 resulted in a drastic reduction in the onset degradation temperature to values below those of neat PLA and the neat blend (refer Table 1 and the insert in Figure 7c). At low clay content (regimes 1 and 2), a higher proportion of the clay was dispersed within the PBSA phase and at the interface and hence, only a small difference was noted between the T_5's of the neat blend and the *regimes 1* and *2* composites. This could be attributed to the fact that a high proportion of the clay resided within the more thermally stable PBSA phase and coupled by the fact that the concentration was very low; their contribution to either improve or affect the onset degradation temperature was minimal.

In contrast, the regime 3 composites have clay particles dispersed within the major matrix, PLA as well. The drastic shift in the T_5 to lower temperatures in this regime signifies that higher concentration of clay promoted early onset of thermal degradation of PLA. Such findings are not unusual for the thermally unstable PLA and a number of authors have reported similar behavior.[28,29] Chang et al.[28] and Wu et al.[29] reported linear reduction in the onset degradation temperatures of PLA nanocomposites with increase in the organoclay loading. No reason was given for this observation but rather, recommendations were made for further study on why there was such decrease in thermal stability. However, in the current study, we postulate that the early onset of degradation of the organic material in the clay as shown in panels a and b in Figure 7 might indeed have resulted in the shift of T_5 of the regime 3 composites to lower temperatures.

The typical first derivative TGA (dTGA) curves shown in Figure 7d−f demonstrate more clearly the difference in thermal stability of the neat PLA and PBSA, their blend, and blend-clay composites. The peaks represent the temperatures at maximum degradation rates. As shown in Figure 7d, the fastest degradation rate typically occurred at 375 °C (average T_{max}= 376 °C, refer to Table 1) for PBSA and at 352 °C for PLA. On blending the two, the fastest degradation rate occurred at a lower temperature (347 °C) than that of neat PLA. The occurrence of a small shoulder in the neat blend dTGA curve, just before the T_{max}, was an indication of immiscibility of the two polymers, with different stages of degradation. The different stages in thermal degradation manifested themselves more clearly in the regime 1 composites as typified by the two peaks in the dTGA curves of B05 as shown in Figure 7e. This was expectedly so, because we recall from the SEM images (see the Supporting Information, Figure S1) that for regime 1 samples, there was an increase in the PBSA dispersed phase sizes when compared to that in the neat blend, signifying phase separation and hence separate stages of thermal degradation unique to the individual polymers. However, in the regime 3 samples, there was a uniform morphology, and indeed, the degradation had a single peak, which shifted to the lower temperatures on increase of clay content.

Overall, the best improvement in thermal stability of the composites over neat blend was realised only in the regimes 1 and 2 composites, when clay content was very low. When clay was in PLA phase, thermal stability was reduced, and this is not a new phenomenon since researchers reported similar reductions in thermal stability of PLA on addition of clay.[28,29] The optimal clay concentration as far as thermal stability is concerned is 2 wt %.

3.4. Tensile Properties. The tensile modulus, yield strength, and elongation at break for the neat PLA, PBSA, neat blend, and blend-clay composites are shown in parts a−c of Figure 8. In addition, for better illustration of the type of failure occurring in the composites, stress-strain graphs of selected specimens was plotted and shown in Figure 9. Regimes 1 and 2 samples had ductile fractures, whereas regime 3 samples had brittle fractures. The neat PLA has much higher modulus than neat PBSA and hence blending the two would expectedly result in lowering of the modulus of the PLA. However, the modulus of the composites tended to increase with an increase in clay content, peaking at around 6 wt %.

Because of their intrinsic high modulus, clays act as rigid reinforcement to the polymer matrix. However, the introduction of a material with a higher modulus cannot be the sole reason for such enhancement in the modulus of the composites. The high aspect ratio of the clay renders a large surface area for the adsorption of the polymers. Apart from this, the intercalation of the polymers into the galleries of clay, on its own, stiffens the polymers. However, such enhancement in modulus with clay may only be realized up to a certain clay loading. Indeed, in the present study, the modulus seemed to peak at 6 wt %, and started to decline on further addition of clay. It is to be noted that reinforcement efficiency of the clay inclusions is only enhanced when there is a proper transfer of the applied stress to the clay platelets. Such transfer of stress is only possible with proper adhesion of the polymers on the clay, which allows the platelets to be load bearing.[30] At higher loading, agglomeration of clay is expected and therefore clay−polymer interaction is reduced. This led to the reduction in the extent of enhancement of reinforcement efficiency with the addition of clay as shown in Figure 8a.

On the other hand, the change in the yield strength and elongation at break was quite different from that of the modulus. The trends in the changes were confined to the different regimes identified earlier: regimes 1, 2, and 3. The regime 1 and 2 samples underwent somewhat ductile fracture, when compared to the brittle fractures observed in regime 3 samples (refer to Figure 9).

In the regime 1, there was a reduction of yield strength and elongation at break on addition of 0.5 wt % clay to the PLA/PBSA blend. However, on further increase in clay loading, the

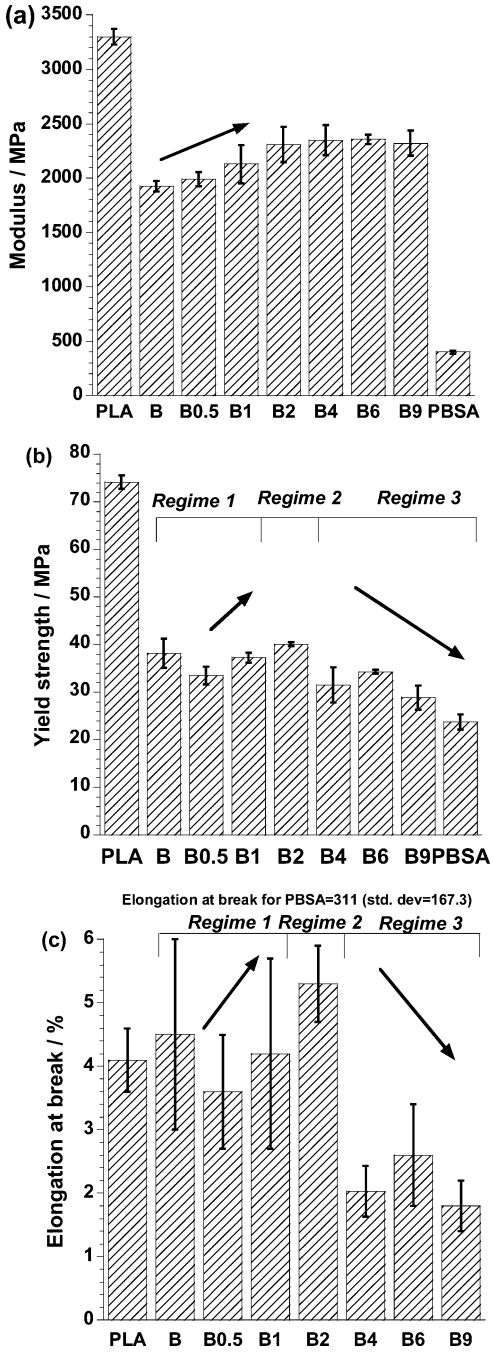

Figure 8. Tensile properties of compression molded and annealed (80 °C for 12 h) samples of neat PLA, PBSA, blend (B) and blend–clay composites (B0.5, B1, B2, B4, B6, and B9, each having 0.5, 1, 2, 4, 6, and 9 wt % clay content, respectively). Reported values are averages of six independent experiments with standard deviations as error bars. The elongation at break of PBSA is 311% (std. dev. = 167.3).

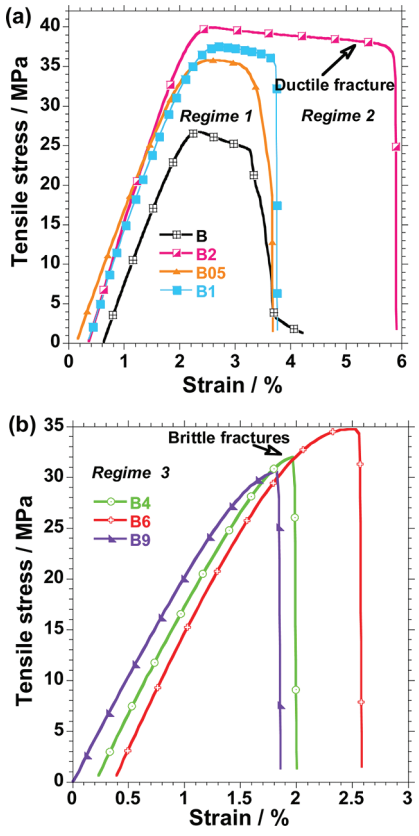

Figure 9. Typical stress–strain curves showing (a) ductile fracture that occurred in the samples: B, B0.5, B1, and B2; and (b) brittle fracture that occurred in the samples: B4, B6, and B9. B, neat blend; B0.5, B1, B2, B4, B6, and B9 are composites with 0.5, 1, 2, 4, 6, and 9 wt % clay, respectively.

yield strength and elongation at break monotonically increased, until a peak was reached at 2 wt %. The yield strength of this transitional regime sample (B2) was ∼5% better than that of the neat blend. Moreover, its elongation at break was ∼18 and ∼29% better than that of neat blend and neat PLA, respectively. This sample (B2) had the best improvement in yield strength and the elongation at break. In the regime 3, further addition of clay resulted in drastic reduction in yield strength and the elongation at break. It is, however, noteworthy to observe that such reduction was not as severe in B6 as compared to that of B4 and B9 samples.

In regime 1, the initial reduction in the yield strength and elongation at break observed in the blend with 0.5 wt % clay when compared to the neat blend could be due to the poorer adhesion between PLA and PBSA phases, as shown by increase in the size of the PBSA phase (refer to supporting information, Figure S1). At 0.5 wt % clay loading, the localized particles within the dispersed PBSA phase were probably not load bearing, because they did not participate in the enhancement of adhesion between the PLA and PBSA phases. However, with the increase in clay loading (B1), more particles were also located at the interface between PLA and PBSA as well as within the PBSA phase (refer to the Supporting Information, Figure S1). This served two purposes: (i) the PBSA phase was stiffened and (ii) clay at the interface helped transfer stress between the PLA and PBSA phases, due to the expected common adsorption of two polymers on clay surface. The net effect was a slight increase in the yield strength and elongation at break, above that of the blend with 0.5 wt % clay content.

For the transitional regime 2, clay particles were found not only within PBSA phase and at the interface but also within PLA. The clay particles within PLA phase, on their own, probably increased the yield strength. However, it is postulated that the main mechanism of the slight improvement in elongation at break for the B2 sample was the clay platelets sitting at the interface between PLA and PBSA. Because of the common adsorption of both polymers on the clay surface, the

clay could be viewed as a bridge between the two phases. Because PBSA has much higher elongation at break than PLA, the load bearing clay at the interface was able to transfer load to the ductile PBSA phase. The net effect was improvement in the elongation at break for the composite. It should be noted that the standard deviation values for the neat blend, blend with 0.5 and 1 wt % clay make the reported differences in the elongation at break insignificant. However, at 2 wt % clay content, a statistically significant difference in elongation at break (when compared to neat PLA) is observed. It is considered that this clay concentration is an important threshold for the PLA/PBSA system in question, when stabilization of morphology of the system starts to occur. With stabilized morphology, come stabilized properties.

In regime 3, sustained clay loading into PLA phase resulted in a statistically significant drastic reduction in yield strength and elongation at break. All the samples within this regime underwent brittle fractures (refer to Figure 9b). This was the expected result since the addition of more clay would result in tactoids and agglomerates within the polymeric matrix. Cracks initiated on and propagated within the clay agglomerates[31,32] resulted in the lower yield strength and elongation at break. The severity in the reduction was not much in B6 when compared to B4 and B9 primarily due to the co-continuous structure in B6.

In conclusion, it is important to note the synergies realized in the sample with 2 wt % clay content. It is unique in that the elongation at break was better than that of neat PLA, even if slightly, without severe reduction in the modulus.

4. CONCLUSIONS

Ternary blends of PLA/PBSA-clay with different clay contents were prepared via melt blending, resulting in composites with different properties. Clay localization and concentration greatly influenced the properties of the composites. At low concentration, clay was located within PBSA phase, primarily due to its lower viscosity when compared to that of PLA at the processing temperature of 185 °C. It has been demonstrated that clay loading and its localization in the PLA/PBSA blend affects the properties of the composites. The most important result in the work was the achievement of a composite (composite with 2 wt.% clay content) with somewhat optimal properties: good mechanical properties with minimal loss of thermal stability. Most importantly, 29% enhancement of the elongation at break over that of neat PLA was achieved. This was attributed to the common adsorption of both polymers onto clay sitting at the interface of PLA and PBSA, thereby acting as a bridge between the two.

■ ASSOCIATED CONTENT

Supporting Information

Detailed scanning and transmission electron microscopic images of PLA/PBSA blend and it organoclay composites; differential scanning calorimetric results of neat PLA and PBSA (PDF). This material is available free of charge via the Internet at http://pubs.acs.org.

■ AUTHOR INFORMATION

Corresponding Author

*Fax: +27 12 841 2229. E-mail: rsuprakas@csir.co.za.

Notes

The authors declare no competing financial interest.

■ ACKNOWLEDGMENTS

The authors (S.S.R. and V.O.) thank the Technology Innovation Agency, South Africa, for financial support and Dr. J. Bandyopadhyay for SAXS measurements.

■ REFERENCES

(1) Amass, W.; Amass, A.; Tighe, B. *Polym. Int.* **1998**, *47*, 89.
(2) Hoshino, A.; Isono, Y. *Biodegradation* **2002**, *13*, 141. Singh, S.; Sinha Ray, S. *J. Nanosci. Nanotechnol.* **2007**, *7*, 2596.
(3) Lee, S.; Lee, J. W. *Korea-Aust. Rheol. J.* **2005**, *17*, 71.
(4) Wu, D.; Zhang, Y.; Zhang, M.; Zhou, W. *Eur. Polym. J.* **2008**, *44*, 2171.
(5) Wang, L.; Ma, W.; Gross, R. A.; McCarthy, S. P. *Polym. Degrad. Stab.* **1998**, *59*, 161.
(6) Wu, D.; Lin, D.; Zhang, J.; Zhou, W.; Zhang, M.; Zhang, Y.; Wang, D.; Lin, B. *Macromol. Chem. Phys.* **2011**, *212*, 613.
(7) Li, Q.; Yoon, J.-S.; Chen, G.-X. *J. Polym. Environ.* **2011**, *19*, 59.
(8) Gu, S.-Y.; Zhang, K.; Ren, J.; Zhan, H. *Carbohy. Polym.* **2008**, *74*, 79.
(9) Wang, Y.; Mano, J. F. *J. Appl. Polym. Sci.* **2007**, *105*, 3204.
(10) Ojijo, V.; Cele, H.; Sinha Ray, S. *Macromol. Mater. Eng.* **2011**, *296*, 865.
(11) Si, M.; Araki, T.; Ade, H.; Kilcoyne, A. L. D.; Fisher, R.; Sokolov, J. C.; Rafailovich, M. H. *Macromolecules* **2006**, *39*, 4793.
(12) Moghbelli, E.; Sue, H.-J.; Jain, S. *Polymer* **2010**, *51*, 4231.
(13) Tao, Y.; Lebovitz, A. H.; Torkelson, J. M. *Polymer* **2005**, *46*, 4753.
(14) Feng, H.; Ye, C.; Tian, J.; Feng, Z.; Huang, B. *Polymer* **1998**, *39*, 1787.
(15) Rhim, J.-W.; Ng, P. K. W. *Crit. Rev. Food Sci. Nutr.* **2007**, *47*, 411. Bordes, P.; Pollet, E.; Avérous, L. *Prog. Mater. Sci.* **2009**, *34*, 125. Paul, D. R.; Robeson, L. M. *Polymer* **2008**, *49*, 3187. Kiliaris, P.; Papaspyrides, C. D. *Prog. Polym. Sci.* **2010**, *35*, 902. Sinha Ray, S.; Okamoto, M. *Prog. Polym. Sci.* **2003**, *28*, 1539. Zou, H.; Wu, S.; Shen, J. *Chem. Rev.* **2008**, *108*, 3893. Hussain, F.; Hojjati, M.; Okamoto, M.; Gorga, R. E. *J. Compos. Mater.* **2006**, *40*, 1511. Alexandre, M.; Dubois, P. *Mater. Sci. Eng. R* **2000**, *28*, 1.
(16) Li, Y.; Simizu, H. *Polymer* **2004**, *45*, 7381. Li, Y.; Shimizu, H. *Macromol. Rapid Commun.* **2005**, *26*, 710. GonzÃlez, I.; EguiazÃbal, J. I.; NazÃbal, J. *Eur. Polym. J.* **2006**, *42*, 2905. Khatua, B. B.; Lee, D. J.; Kim, H. Y.; Kim, J. K. *Macromolecules* **2004**, *37*, 2454.
(17) Sinha Ray, S.; Pouliot, S.; Bousmina, M.; Utracki, L. A. *Polymer* **2004**, *45*, 8403. Sinha Ray, S.; Bousmina, M. *Macromol. Rapid Commun.* **2005**, *26*, 450. Sinha Ray, S.; Bousmina, M. *Macromol. Rapid Commun.* **2005**, *26*, 1639. Sinha Ray, S.; Bandyopadhyay, J.; Bousmina, M. *Macromol. Mater. Eng.* **2007**, *92*, 729.
(18) Yu, Z.; Yin, J.; Yan, S.; Xie, Y.; Ma, J.; Chen, X. *Polymer* **2007**, *48*, 6439.
(19) Chen, G.-X.; Kim, H.-S.; Kim, E.-S.; Yoon, J.-S. *Polymer* **2005**, *46*, 11829.
(20) Chen, G.-X.; Yoon, J.-S. *J. Polym. Sci., Part B: Polym. Phys.* **2005**, *43*, 478.
(21) Wu, D.; Zhang, Y.; Zhang, M.; Yu, W. *Biomacromolecules* **2009**, *10*, 417.
(22) Southern Clay Products Inc.: Gonzales, TX.
(23) Ojijo, V.; Malwela, T.; Sinha Ray, S.; Sadiku, R. *Polymer* **2012**, *53*, 505.
(24) Mezger, T. G. *The Rheology Handbook*, 2nd ed.; Vincentz Network GmbH & Co.: Hannover, Germany, 2006.
(25) Tol, R. T.; Mathot, V. B. F.; Reynaers, H.; Goderis, B.; Groeninckx, G. *Polymer* **2005**, *46*, 2966.
(26) Balsamo, V.; Gouveia, L. M. *J. Polym. Sci., Part B: Polym. Phys.* **2007**, *45*, 1365.
(27) Sinha Ray, S.; Okamoto, M. *Prog. Mater. Sci.* **2003**, *28*, 1539.
(28) Chang, J.-H.; An, Y. U.; Cho, D.; Giannelis, E. P. *Polymer* **2003**, *44*, 3715.
(29) Wu, D.; Wu, L.; Wu, L.; Zhang, M. *Polym. Degrad. Stab.* **2006**, *91*, 3149.

(30) Shia, D.; Hui, C. Y.; Burnside, S. D.; Giannelis, E. P. *Polym. Compos.* **1998**, *19*, 608.
(31) Kim, G. M.; Lee, D. H.; Hoffmann, B.; Kressler, J.; Stöppelmann, G. *Polymer* **2001**, *42*, 1095.
(32) Masenelli-Varlot, K.; Reynaud, E.; Vigier, G.; Varlet, J. *J. Polym. Sci., Part B: Polym. Phys.* **2002**, *40*, 272.